

Supramolecular association in proton-transfer adducts containing benzamidine cations. I. Four molecular salts with uracil derivatives

Gustavo Portalone

Chemistry Department, 'Sapienza' University of Rome, Piazzale A. Moro 5,
I-00185 Rome, Italy
Correspondence e-mail: g.portalone@caspur.it

Received 3 March 2010

Accepted 3 May 2010

Online 13 May 2010

Four organic salts, namely benzamidine orotate (2,6-dioxo-1,2,3,6-tetrahydropyrimidine-4-carboxylate) hemihydrate, $C_7H_9N_2^+ \cdot C_5H_3N_2O_4^- \cdot 0.5H_2O$ (BenzamH⁺·Or⁻), (I), benzamidine isoorotate (2,4-dioxo-1,2,3,4-tetrahydropyrimidine-5-carboxylate) trihydrate, $C_7H_9N_2^+ \cdot C_5H_3N_2O_4^- \cdot 3H_2O$ (BenzamH⁺·Isor⁻), (II), benzamidine diliturate (5-nitro-2,6-dioxo-1,2,3,6-tetrahydropyrimidin-4-olate) dihydrate, $C_7H_9N_2^+ \cdot C_4H_2N_3O_5^- \cdot 2H_2O$ (BenzamH⁺·Dil⁻), (III), and benzamidine 5-nitrouracilate (5-nitro-2,4-dioxo-1,2,3,4-tetrahydropyrimidin-1-ide), $C_7H_9N_2^+ \cdot C_4H_2N_3O_4^-$ (BenzamH⁺·Nit⁻), (IV), have been synthesized by a reaction between benzamidine (benzenecarboximidamide or Benzam) and the appropriate carboxylic acid. Proton transfer occurs to the benzamidine imino N atom. In all four acid–base adducts, the asymmetric unit consists of one tautomeric amino oxo anion (Or⁻, Isor⁻, Dil⁻ and Nit⁻) and one monoprotonated benzamidine cation (BenzamH⁺), plus one-half (which lies across a twofold axis), three and two solvent water molecules in (I), (II) and (III), respectively. Due to the presence of protonated benzamidine, these acid–base complexes form supramolecular synthons characterized by N⁺–H···O⁻ and N⁺–H···N⁻ (±)-charge-assisted hydrogen bonds (CAHB).

Comment

An invaluable approach for supramolecular synthesis is the exploitation of the principles of molecular self-assembly. This relies heavily on the ability of certain functional groups to self-interact in a noncovalent fashion and to retain a specific and persistent pattern or motif, the supramolecular synthon. Among the functional groups used most frequently for supramolecular synthesis and crystal engineering are carboxyl groups and their derivatives. These functions are capable of forming robust and directional hydrogen bonds, and aggregate in the solid state as dimers, catemers and double-bridged motifs (Leiserowitz, 1976; Bernstein *et al.*, 1994; Kolotuchin *et*

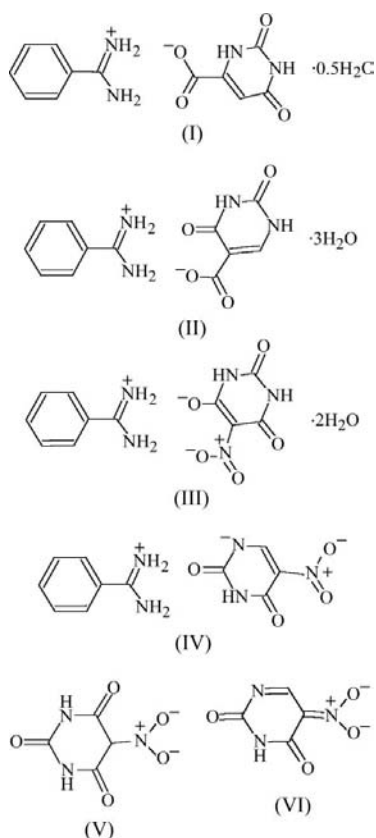
al., 1995), allowing reasonably good control over the resulting structures.

It has been observed that the strength of directional forces depends on the nature and polarity of the donor and acceptor groups. Enhancement of hydrogen-bond strength by resonance or ionic charge has long been recognized (Ferretti *et al.*, 2004; Ward, 2005; Kojić-Prodić & Molčanov, 2008, and references therein). The protonated form of benzamidine appears to be a very promising building block in supramolecular chemistry because its multiple hydrogen-bond donors can interact with anions having multiple acceptor sites, such as carboxylates. Although it is difficult to predict the formation of a hydrogen bond between a potential donor *D*–H group and a potential acceptor *A* in a given system, a probability of formation (P_m) can be defined. This is the fraction of *D*–H···*A* hydrogen bonds (or hydrogen-bond arrays) out of the total number of such hydrogen bonds that could be formed. From the probabilities of formation of 75 bimolecular ring motifs that have been determined (Allen *et al.*, 1999), the rather poor performance of the amidinium–carboxylate heterodimer ($P_m = 0.51$) can be explained by strong competition of alternative motifs. In contrast, in the case of salts containing the benzamidine cation, although only a few structures have been reported, the $R_2^2(8)$ (Etter *et al.*, 1990; Bernstein *et al.*, 1995; Motherwell *et al.*, 1999) one-dimensional heterosynthon with carboxylate or other oxygenate anions predominates (Kratochvíl *et al.*, 1987; Portalone, 2008a; Kolev *et al.*, 2009). These acid–base complexes are usually arranged in a dimeric motif, similar to that found in carboxylic acid dimers, *via* N⁺–H···O⁻ (±)-charge-assisted hydrogen bonds (CAHB) (Gilli & Gilli, 2009), provided that ΔpK_a [$\Delta pK_a = pK_a(\text{base}) - pK_a(\text{acid})$, where the pK_a are for aqueous solutions] is sufficiently large. The value of ΔpK_a is often used to predict whether a salt or cocrystal can be expected for two components (Johnson & Rumon, 1965; Childs *et al.*, 2007), but some exceptions have been reported (Herbstein, 2005; Molčanov & Kojić-Prodić, 2010). A value of $\Delta pK_a < 0$ is generally considered to be associated with systems that form cocrystals, $\Delta pK_a > 3$ results in salts, while $0 < \Delta pK_a < 3$ can produce cocrystals, salts or mixed ionization complexes.

Another possibility is offered by coupling benzamidine cations with counter-ions containing the NO₂ group as hydrogen-bond acceptor in complementary bimolecular (DD)·(AA) heterosynthons. Although nitro groups are intrinsically poorer acceptors of hydrogen bonds than carboxylates (Gagnon *et al.*, 2007), they form a variety of weak supramolecular synthons with different types of donors (*e.g.* O–H, aniline N–H, C≡C–H and C–Hal) (Robinson *et al.*, 2000; Thallapally *et al.*, 2003; Thomas *et al.*, 2005). Consequently, the preference of a particular class of donor, such as the protonated analogues of benzamidine, to form symmetric motifs with nitro groups could rely on the characteristics of the hydrogen-bond donor.

In this study, an analysis of solid-state heteromeric and homomeric hydrogen-bond interactions has been carried out on four acid–base complexes formed by benzamidine (Benzam) with orotic acid (Or), isoorotic acid (Isor), dilituric

acid (Dil) and 5-nitrouracil (Nit). Benzamidine derivatives such as pentamidine and propamidine are very simple DNA binders that show good stability, A/T sequence selectivity, and excellent cell-transport properties in a variety of cell lines (Tidwell & Boykin, 2003). Benzamidine itself also has biological and pharmacological relevance (Powers & Harper, 1999; Grzesiak *et al.*, 2000). With this in mind, the acids Or, Isor, Dil and Nit were selected to react with benzamidine as they possess appreciable acidity and are structurally related to thymine (2,4-dihydroxy-5-methylpyrimidine). In these four complexes, (I)–(IV), the ΔpK_a values are 9.5, 7.4, 10.8 and 5.9, respectively, so salts are expected. In situations where both anion and cation are derived from organic acids and bases, the term molecular salt has been proposed (Sarma *et al.*, 2009).



In these four 1:1 proton-transfer compounds, protonation occurs at the benzamidine imino N atom as a result of proton transfer from the acidic hydroxy [compounds (I)–(III)] and amino groups [compound (IV)]. These acid–base complexes are linked by $N^+ - H \cdots O^-$ and $N^+ - H \cdots N^- (\pm)$ -CAHB. The amidinium fragments are completely delocalized (Table 1) and can be described as carrying a half-positive formal charge on the two N atoms. The same delocalization occurs within the carboxylate group in $BenzamH^+ \cdot Or^-$, (I), and favours aggregation into dimers. In $BenzamH^+ \cdot Isor^-$, (II), and $BenzamH^+ \cdot Dil^-$, (III), the lack of hydrogen-bond acceptors with respect to imino hydrogen-bond donors gives rise to the formation of bifurcated hydrogen bonds.

Compound (I) crystallizes in the monoclinic space group $C2/c$, with one tautomeric aminooxo anion (Or^-), one monoprotonated benzamidine cation ($BenzamH^+$) and

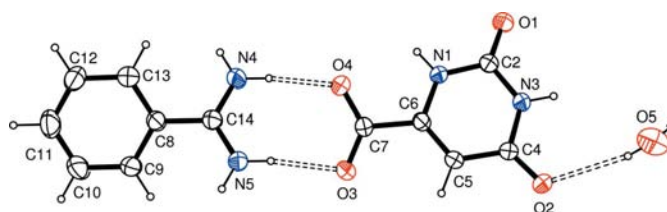


Figure 1

The asymmetric unit of (I), showing the atom-labelling scheme and hydrogen bonding (dashed lines). The asymmetric unit was selected so that the two ions are linked by $N^+ - H \cdots O^- (\pm)$ -CAHB hydrogen bonds. Displacement ellipsoids are drawn at the 50% probability level and H atoms are shown as small spheres of arbitrary radii.

one-half of a solvent water molecule (which lies across a twofold axis) in the asymmetric unit (Fig. 1). The $BenzamH^+$ cation is not planar. The amidinium group has a synclinal disposition with respect to the benzene ring [N4–C14–C8–C13 and N5–C14–C8–C9 torsion angles are 29.3 (2) and 29.2 (2)°, respectively], close to the values observed in benzamidine [22.7 (3) and 20.9 (3)°; Barker *et al.*, 1996] and benzdiamidine [25.3 (2) and 23.8 (2)°; Jokić *et al.*, 2001]. This disposition is a consequence of an overcrowding effect, *i.e.* steric hindrance between the H atoms of the aromatic ring and the amidine moiety. In the Or^- anion, the pyrimidine ring is essentially planar and the carboxylate group is rotated 15.4 (2)–15.7 (2)° out of the plane of the uracil fragment. For this anion, the bond lengths and angles of the heteroaromatic ring are in accord with values obtained for orotic acid monohydrate (Portalone, 2008*b*). The two ions are joined by two $N^+ - H \cdots O^- (\pm)$ -CAHB hydrogen bonds to form a dimer with graph-set motif $R_2^2(8)$ (Table 2).

Compound (II) crystallizes in the monoclinic space group $P2_1/n$, with one almost planar tautomeric aminooxo anion ($Isor^-$), one $BenzamH^+$ cation and three solvent water molecules in the asymmetric unit (Fig. 2). In the nonplanar $BenzamH^+$ cation, the amidinium group is twisted out of the

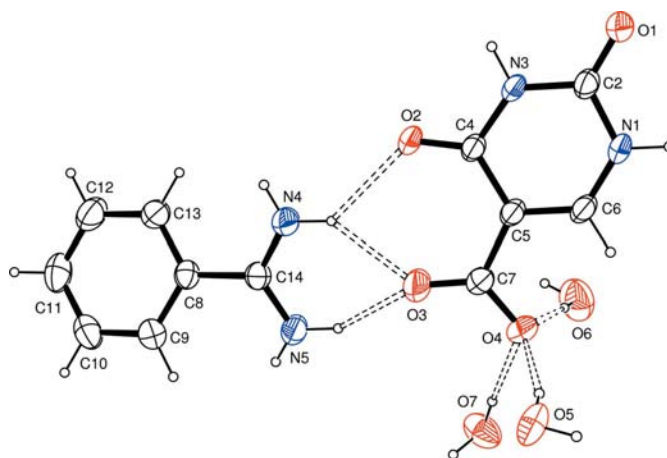


Figure 2

The asymmetric unit of (II), showing the atom-labelling scheme and hydrogen bonding (dashed lines). The asymmetric unit was selected so that the two ions are linked by $N^+ - H \cdots O^- (\pm)$ -CAHB hydrogen bonds. Displacement ellipsoids are drawn at the 50% probability level and H atoms are shown as small spheres of arbitrary radii.

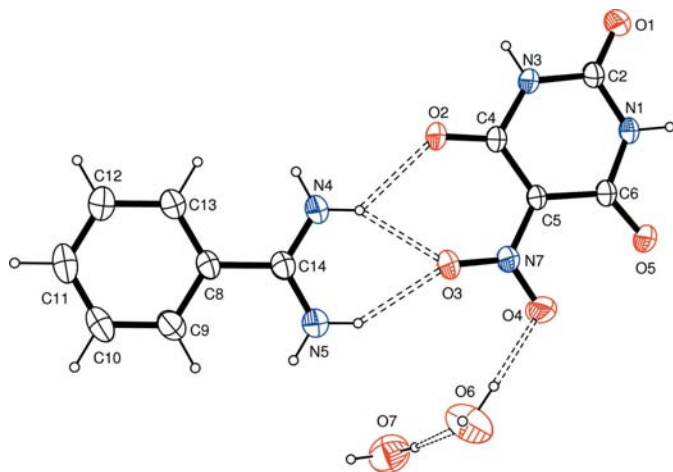


Figure 3

The asymmetric unit in (III), showing the atom-labelling scheme and hydrogen bonding (dashed lines). The asymmetric unit was selected so that the two ions are linked by $N^+ - H \cdots O^- (\pm)$ -CAHB hydrogen bonds. Displacement ellipsoids are drawn at the 50% probability level and H atoms are shown as small spheres of arbitrary radii.

mean plane of the benzene ring [N4–C14–C8–C13 and N5–C14–C8–C9 torsion angles are 23.2 (3) and 22.5 (3)°, respectively]. Comparison of the geometric parameters of the Isor[−] anion in (II) with those reported for the isoorotate anion in the 1:1 proton-transfer adduct between cytosine and isoorotic acid (Portalone & Colapietro, 2009) shows that the corresponding bond lengths and angles are equal within experimental error. The two ions are connected by three $N^+ - H \cdots O^- (\pm)$ -CAHB hydrogen bonds, which include one bifurcated donor and one bifurcated acceptor interaction. The Isor[−] anion accepts two of these hydrogen bonds through one O atom of the carboxylate group and the third through the adjacent carbonyl O atom. These interactions generate graph-set motifs of $R_2^1(6)$ and $R_2^2(6)$ (Table 3).

Compound (III) also crystallizes in the monoclinic space group $P2_1/n$, with one planar tautomeric aminooxo anion (Dil[−]), one BenzamH⁺ cation and two solvent water molecules in the asymmetric unit (Fig. 3). At variance with adducts (I) and (II), in (III) the BenzamH⁺ cation is planar [N4–C14–C8–C13 and N5–C14–C8–C9 torsion angles are 0.5 (2) and 0.7 (2)°, respectively]. This conformation is rather unusual, as only the nonplanar arrangement has been observed in previous small-molecule structures. Quite the opposite is true in benzamidinium-containing macromolecular structures, in which the most frequently encountered conformation is the planar one (Li *et al.*, 2009). In the planar Dil[−] anion, the release of an H atom from the hydroxy O atom causes a redistribution of π -electron density so that the geometry of the anion (Table 1) approaches mirror symmetry through a mirror plane along the line joining atoms C2 and C5 [form (V)]. As with the previous case, the two ions are connected by bifurcated $N^+ - H \cdots O^- (\pm)$ -CAHB hydrogen bonds, which generate $R_2^1(6)$ and $R_2^2(6)$ motifs, but the Dil[−] anion acts as an acceptor through one O atom of the nitro group and the adjacent carbonyl O atom (Table 4). A similar hydrogen-bond pattern has been observed in the 1:1 salts of

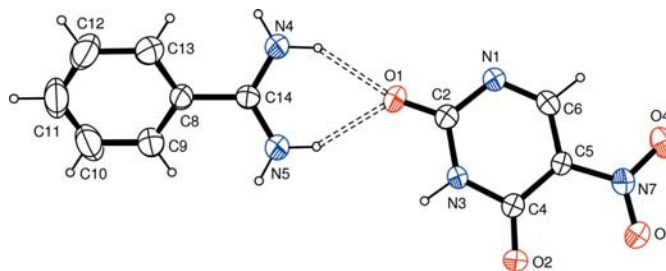


Figure 4

The asymmetric unit in (IV), showing the atom-labelling scheme and hydrogen bonding (dashed lines). The asymmetric unit was selected so that the two ions are linked by $N^+ - H \cdots O$ hydrogen bonds. Displacement ellipsoids are drawn at the 50% probability level and H atoms are shown as small spheres of arbitrary radii.

phenylbiguanide and dilituric acid monohydrate (Portalone & Colapietro, 2007a).

Compound (IV) crystallizes in the triclinic space group $P\bar{1}$, with one planar tautomeric aminooxo anion (Nit[−]) and one BenzamH⁺ cation in the asymmetric unit (Fig. 4). Again, the BenzamH⁺ cation is not planar. The amidinium group, as in (I), has a synclinal disposition with respect to the benzene ring [N4–C14–C8–C13 and N5–C14–C8–C9 torsion angles are 29.7 (4) and 30.4 (3)°, respectively]. Of the two sites available for ionization in the heterocyclic ring of the 5-nitrouracil molecule (N1 and N3), deprotonation occurs at the more acidic N1 (Portalone & Colapietro, 2007b), and this causes a redistribution of π -electron density in the Nit[−] anion. The resulting distortions in the molecular geometry of the anion (Table 1), which have been observed in the only reported structure containing the 5-nitrouracilate unit (Pereira Silva *et al.*, 2008), point to the importance of the charge-separated quinoid form (VI) as a significant contributor. The two ions are connected by two $N^+ - H \cdots O$ hydrogen bonds, and the carbonyl atom O1 of the Nit[−] anion acts as a bifurcated acceptor, thus generating an $R_2^1(6)$ motif (Table 5).

As previously mentioned, due to their protonated base, the supramolecular aggregations in compounds (I)–(IV) are dominated by an extensive series of hydrogen bonds, which include $N^+ - H \cdots O$, $N^+ - H \cdots O^-$ and $N^+ - H \cdots N^- (\pm)$ -CAHB hydrogen bonds. Analysis of the resulting supramolecular structures is greatly eased by the use of the substructure approach (Gregson *et al.*, 2000), as in each of (I)–(IV) it is possible to identify a basic structural subunit built from the ion pairs of the asymmetric unit.

In the supramolecular structure of (I), which is a stoichiometric hemihydrate, seven hydrogen bonds link the molecular components into a three-dimensional framework structure (Table 2). One subunit generates a centrosymmetric $R_2^2(8)$ hydrogen-bonding motif. Two centrosymmetric subunits are then linked into a two-dimensional network *via* multiple hydrogen bonds, forming two adjoining hydrogen-bonded rings with graph-set motifs $R_3^3(14)$ and $R_4^4(18)$. The formation of the final three-dimensional array is facilitated by the water molecules, which act as bridges between structural subunits linked into $R_4^3(12)$ hydrogen-bonded rings (Fig. 5).

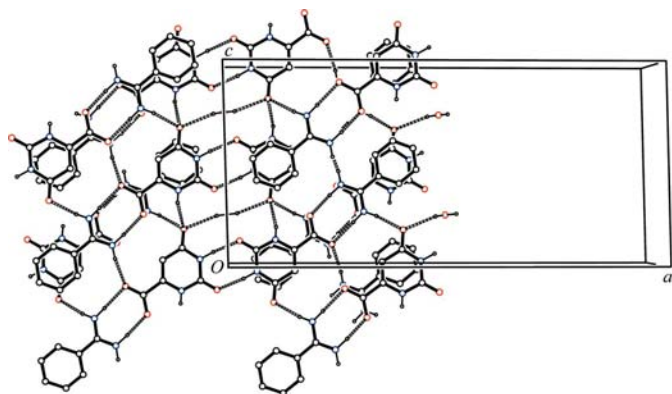


Figure 5
A crystal packing diagram for (I), viewed approximately down the *b* axis. All atoms are shown as small spheres of arbitrary radii. For the sake of clarity, carbon-bound H atoms have been omitted. Hydrogen bonding is indicated by dashed lines.

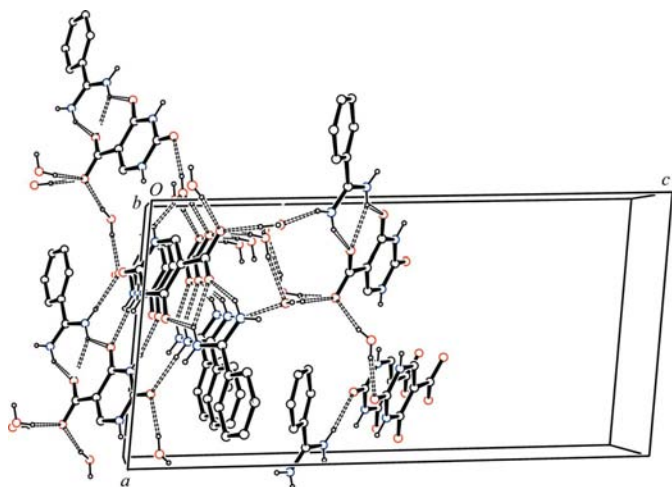


Figure 6
A crystal packing diagram for (II), viewed approximately down the *b* axis. All atoms are shown as small spheres of arbitrary radii. For the sake of clarity, carbon-bound H atoms have been omitted. Hydrogen bonding is indicated by dashed lines.

In the crystal structure of (II), which is a stoichiometric trihydrate, the hydrogen-bonding scheme is rather complex and involves all available hydrogen donor and acceptor sites. In total, the supramolecular structure of (II) is characterized by 13 hydrogen bonds, namely seven $N-H\cdots O$ and six $O-H\cdots O$ bonds (Table 3). Two coplanar subunits form centrosymmetric $R_2^2(8)$ and $R_3^3(8)$ rings *via* double intermolecular $N^+-H\cdots O$ and $N-H\cdots O$ hydrogen bonds. These pairs further self-organize through double intermolecular $OW-H\cdots O$ hydrogen bonds with a water molecule, to generate infinite chains of rings running approximately parallel to the [100] direction (Fig. 6). The hydrogen bonds so far discussed in the two-dimensional arrays in the *ac* plane are bridged by the remaining water molecules *via* $OW-H\cdots O$ interactions.

From a topological point of view, the crystal structure of (III), which is a stoichiometric dihydrate, shows similarities with that of (II). Two coplanar subunits form centrosymmetric $R_2^2(8)$ and $R_3^3(8)$ rings *via* intermolecular $N^+-H\cdots O$ and $N-$

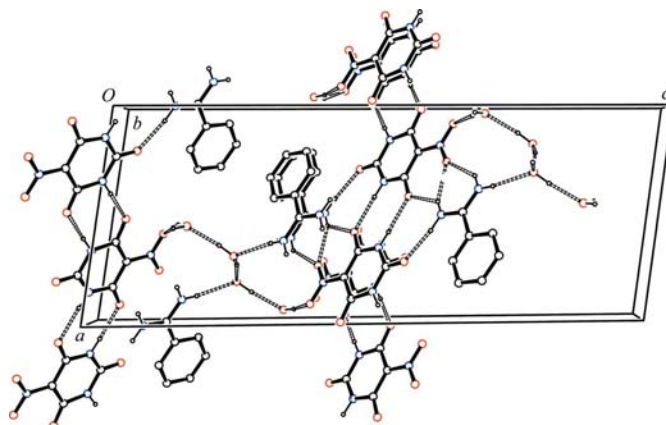


Figure 7
A crystal packing diagram for (III), viewed approximately down the *b* axis. All atoms are shown as small spheres of arbitrary radii. For the sake of clarity, carbon-bound H atoms have been omitted. Hydrogen bonding is indicated by dashed lines.

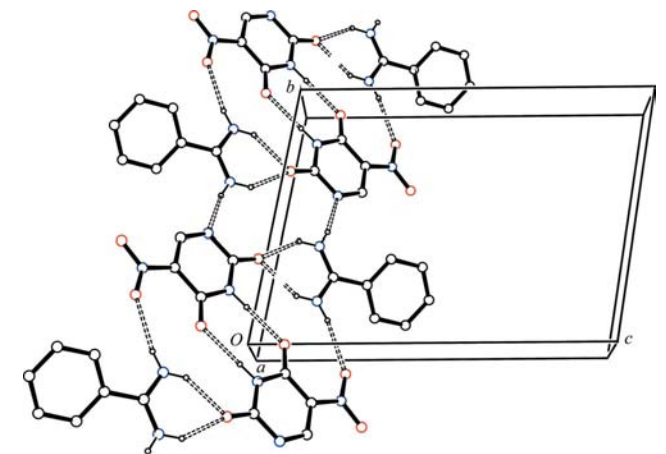


Figure 8
Part of the crystal structure of (IV), showing the formation of a hydrogen-bonded ribbon approximately along [110]. All atoms are shown as small spheres of arbitrary radii. For the sake of clarity, carbon-bound H atoms have been omitted. Hydrogen bonding is indicated by dashed lines.

$H\cdots O$ hydrogen bonds. In this case, however, these pairs further self-organize through an intermolecular $R_2^2(8)$ $N-H\cdots O$ interaction formed around an inversion centre, giving infinite chains of rings running approximately parallel to the [100] direction. The formation of this two-dimensional array is then reinforced by two water molecules (Fig. 7).

The molecules of (IV) are linked by a combination of five $N^+-H\cdots O$ and $N^+-H\cdots N^-(\pm)$ -CAHB (Table 5). Neighbouring subunits form a sheet-like structure *via* three structurally significant hydrogen bonds (Fig. 8). Two centrosymmetric subunits are linked by two independent $N^+-H\cdots O$ hydrogen bonds, forming fused centrosymmetric rings with graph-set motifs $R_3^3(12)$ and $R_2^2(8)$. An $N^+-H\cdots N^-(\pm)$ homonuclear (\pm)-CAHB then connects these two subunits to produce an adjoining centrosymmetric $R_4^4(12)$ ring. Propagation by inversion of these subunits suffices to link all the molecules into a ribbon approximately along [110].

From a supramolecular retrosynthesis perspective, only those synthons that occur repeatedly in crystal structures, namely robust synthons of a particular set of functional groups, are useful in crystal design (Nangia & Desiraju, 1998). Moreover, hydrogen bonds are often formed in a hierarchical fashion (Etter, 1990; Allen *et al.*, 1999; Bis *et al.*, 2007; Shattock *et al.*, 2008), and there is a need to ascertain the prevalence of a particular heterosynthon over another in a competitive environment. From the results reported here, only the crystal structure of (I) is consistent with the $R_2^2(8)$ supramolecular heterosynthon persistence exhibited by the benzamidine adducts that have been archived in the Cambridge Structural Database (CSD, Version 5.30; Allen, 2002). Consequently, it would be of interest to pursue crystal engineering studies that provide possible correlations between the synthons used and the topology of the hydrogen bonds in benzamidine-containing molecular salts. Moreover, such proton-transfer adducts are ideally suited to studying the competition between different supramolecular heterosynthons if the counter-ions in benzamidine salts are from molecules having acceptor groups whose nature is modified in a graded manner through chemical synthesis. Work in this laboratory has begun to tackle this issue, and a systematic analysis of the structural consequences for solid-state assembly in benzamidine proton-transfer adducts as a function of the hydrogen-bond acceptor properties of the coupling agents is currently under investigation.

Experimental

BenzamH⁺·Or⁻, (I), BenzamH⁺·Isor⁻, (II), BenzamH⁺·Dil⁻, (III), and BenzamH⁺·Nit⁻, (IV), were obtained as white powders from equimolar mixtures (1 mmol of each compound) in ethanol solutions (20 ml) of benzamidine (Fluka, 95%) and ototic acid (Sigma Aldrich, 98%), isoorotic acid (Sigma Aldrich, 95%), dilituric acid (Sigma Aldrich, 95%) and 5-nitrouacil (Sigma Aldrich, 98%), respectively. The 1:1 molecular adducts were recrystallized from water. The solutions were warmed slowly and then left to evaporate under ambient conditions. Small transparent single crystals were deposited after two weeks.

Compound (I)

Crystal data

$C_7H_9N_2^+ \cdot C_5H_3N_2O_4^- \cdot 0.5H_2O$
 $M_r = 285.27$

Monoclinic, $C2/c$
 $a = 27.2046$ (6) Å
 $b = 7.3566$ (2) Å
 $c = 12.6687$ (3) Å
 $\beta = 91.621$ (2)°

$V = 2534.41$ (11) Å³
 $Z = 8$

Mo $K\alpha$ radiation
 $\mu = 0.12$ mm⁻¹
 $T = 298$ K
 $0.30 \times 0.20 \times 0.15$ mm

Data collection

Oxford Xcalibur S CCD area-detector diffractometer
 Absorption correction: multi-scan [CrysAlis RED (Oxford Diffraction, 2006); empirical (using intensity measurements) absorption correction using spherical harmonics implemented

in the SCALE3 ABSPACK scaling algorithm]
 $T_{\min} = 0.956$, $T_{\max} = 0.983$
 119911 measured reflections
 4342 independent reflections
 3512 reflections with $I > 2\sigma(I)$
 $R_{\text{int}} = 0.043$

Refinement

$R[F^2 > 2\sigma(F^2)] = 0.065$
 $wR(F^2) = 0.152$
 $S = 1.20$
 4342 reflections
 214 parameters

H atoms treated by a mixture of independent and constrained refinement
 $\Delta\rho_{\text{max}} = 0.36$ e Å⁻³
 $\Delta\rho_{\text{min}} = -0.18$ e Å⁻³

Compound (II)

Crystal data

$C_7H_9N_2^+ \cdot C_5H_3N_2O_4^- \cdot 3H_2O$
 $M_r = 330.30$
 Monoclinic, $P2_1/n$
 $a = 11.3562$ (2) Å
 $b = 6.0402$ (1) Å
 $c = 22.3763$ (4) Å
 $\beta = 96.221$ (2)°

$V = 1525.84$ (5) Å³
 $Z = 4$
 Mo $K\alpha$ radiation
 $\mu = 0.12$ mm⁻¹
 $T = 298$ K
 $0.18 \times 0.14 \times 0.09$ mm

Data collection

Oxford Xcalibur S CCD area-detector diffractometer
 Absorption correction: multi-scan [CrysAlis RED (Oxford Diffraction, 2006); empirical (using intensity measurements) correction using spherical harmonics

implemented in the SCALE3 ABSPACK scaling algorithm]
 $T_{\min} = 0.918$, $T_{\max} = 0.990$
 218566 measured reflections
 5260 independent reflections
 3884 reflections with $I > 2\sigma(I)$
 $R_{\text{int}} = 0.073$

Table 1

Selected bond distances (Å) for (I)–(IV).

Bond	(I)	(II)	(III)	(IV)
O1–C2	1.2179 (16)	1.225 (2)	1.2215 (18)	1.232 (3)
O2–C4	1.2289 (16)	1.2293 (19)	1.2364 (16)	1.224 (3)
O3–C7	1.2483 (15)	1.230 (2)		
O4–C7	1.2400 (17)	1.273 (2)		
O3–N7			1.2385 (16)	1.229 (2)
O4–N7			1.2364 (17)	1.232 (2)
O5–C6			1.2287 (17)	
N1–C2	1.3664 (16)	1.370 (2)	1.3605 (18)	1.366 (3)
N1–C6	1.3673 (16)	1.352 (2)	1.3848 (18)	1.316 (3)
N3–C2	1.3717 (18)	1.371 (2)	1.3652 (17)	1.371 (3)
N3–C4	1.3765 (16)	1.389 (2)	1.3835 (17)	1.382 (3)
C4–C5	1.4431 (17)	1.455 (2)	1.4416 (18)	1.443 (3)
C5–C6	1.3385 (18)	1.355 (2)	1.4478 (17)	1.381 (3)
C5–C7		1.500 (2)		
C5–N7			1.3945 (17)	1.421 (3)
C6–C7	1.5225 (17)			
N4–C14	1.3118 (17)	1.318 (2)	1.3083 (19)	1.309 (3)
N5–C14	1.3106 (18)	1.312 (2)	1.321 (2)	1.302 (3)
C8–C14	1.4763 (18)	1.483 (2)	1.4843 (19)	1.478 (3)
C8–C9	1.3901 (18)	1.395 (3)	1.391 (2)	1.384 (3)
C8–C13	1.386 (2)	1.393 (3)	1.389 (2)	1.387 (4)
C9–C10	1.386 (2)	1.387 (3)	1.389 (2)	1.375 (4)
C12–C13	1.386 (2)	1.384 (3)	1.386 (2)	1.394 (4)
C10–C11	1.377 (3)	1.376 (3)	1.377 (3)	1.368 (4)
C11–C12	1.375 (2)	1.379 (3)	1.372 (3)	1.373 (5)

Table 2

Hydrogen-bond geometry (Å, °) for (I).

$D-H \cdots A$	$D-H$	$H \cdots A$	$D \cdots A$	$D-H \cdots A$
N1–H1 ⁱ ···O2 ⁱ	0.82 (2)	2.24 (2)	3.0013 (16)	153.5 (18)
N3–H3 ⁱ ···O1 ⁱⁱ	0.96 (2)	1.90 (2)	2.8491 (15)	168.0 (19)
N4–H4A ⁱ ···O4	0.97 (2)	1.82 (2)	2.7809 (16)	170.6 (18)
N4–H4B ⁱ ···O3 ⁱ	0.91 (2)	2.00 (2)	2.9036 (17)	171.4 (18)
N5–H5A ⁱ ···O3	0.92 (2)	1.95 (2)	2.8638 (16)	178 (2)
N5–H5B ⁱ ···O2 ⁱⁱⁱ	0.89 (2)	2.06 (2)	2.9357 (16)	170.0 (17)
O5–H51 ⁱ ···O2	0.85 (3)	2.35 (3)	3.1345 (14)	154 (3)

Symmetry codes: (i) $x, -y + 1, z + \frac{1}{2}$; (ii) $-x, -y + 1, -z$; (iii) $-x + \frac{1}{2}, -y + \frac{1}{2}, -z$.

Table 3
Hydrogen-bond geometry (Å, °) for (II).

D—H...A	D—H	H...A	D...A	D—H...A
N1—H1...O5 ⁱ	0.92 (3)	2.05 (3)	2.760 (2)	133 (2)
N3—H3...O2 ⁱⁱ	0.89 (3)	1.95 (3)	2.8296 (18)	174 (2)
N4—H4A...O2	0.92 (3)	2.22 (3)	2.959 (2)	136 (2)
N4—H4A...O3	0.92 (3)	2.08 (3)	2.854 (2)	141 (2)
N4—H4B...O1 ⁱⁱⁱ	0.84 (3)	2.24 (3)	3.050 (2)	162 (2)
N5—H5A...O3	0.92 (3)	1.92 (3)	2.770 (2)	154 (2)
N5—H5B...O7 ⁱⁱⁱ	0.88 (3)	2.03 (3)	2.868 (2)	158 (2)
O5—H51...O4	0.90 (4)	1.91 (4)	2.787 (2)	163 (3)
O5—H52...O1 ^{iv}	0.83 (3)	2.00 (3)	2.821 (2)	173 (3)
O6—H61...O4	0.91 (4)	1.94 (4)	2.837 (3)	171 (3)
O6—H62...O7 ^v	0.80 (4)	2.09 (4)	2.878 (3)	169 (4)
O7—H71...O4	0.86 (3)	1.89 (3)	2.741 (2)	173 (3)
O7—H72...O6 ^{vi}	0.84 (3)	1.88 (3)	2.704 (3)	166 (3)

Symmetry codes: (i) $x, y + 1, z$; (ii) $-x + 1, -y + 2, -z$; (iii) $-x + \frac{1}{2}, y - \frac{1}{2}, -z + \frac{1}{2}$ (iv) $-x, -y + 2, -z$; (v) $-x + \frac{1}{2}, y + \frac{1}{2}, -z + \frac{1}{2}$; (vi) $x, y - 1, z$.

Refinement

$R[F^2 > 2\sigma(F^2)] = 0.087$
 $wR(F^2) = 0.186$
 $S = 1.24$
 5260 reflections
 256 parameters
 H atoms treated by a mixture of independent and constrained refinement
 $\Delta\rho_{\max} = 0.36 \text{ e } \text{Å}^{-3}$
 $\Delta\rho_{\min} = -0.25 \text{ e } \text{Å}^{-3}$

Compound (III)

Crystal data

$\text{C}_7\text{H}_9\text{N}_2^+ \cdot \text{C}_4\text{H}_2\text{N}_3\text{O}_5^- \cdot 2\text{H}_2\text{O}$
 $M_r = 329.28$
 Monoclinic, $P2_1/n$
 $a = 10.7607 (3) \text{ Å}$
 $b = 5.0998 (2) \text{ Å}$
 $c = 27.2412 (5) \text{ Å}$
 $\beta = 98.2485 (11)^\circ$
 $V = 1479.46 (8) \text{ Å}^3$
 $Z = 4$
 Mo $K\alpha$ radiation
 $\mu = 0.13 \text{ mm}^{-1}$
 $T = 298 \text{ K}$
 $0.16 \times 0.14 \times 0.12 \text{ mm}$

Data collection

Oxford Xcalibur S CCD area-detector diffractometer
 Absorption correction: multi-scan [CrysAlis RED (Oxford Diffraction, 2006); empirical (using intensity measurements) absorption correction using spherical harmonics implemented
 in the SCALE3 ABSPACK scaling algorithm
 $T_{\min} = 0.908, T_{\max} = 0.991$
 306312 measured reflections
 5116 independent reflections
 4542 reflections with $I > 2\sigma(I)$
 $R_{\text{int}} = 0.034$

Refinement

$R[F^2 > 2\sigma(F^2)] = 0.064$
 $wR(F^2) = 0.165$
 $S = 1.17$
 5116 reflections
 248 parameters
 H atoms treated by a mixture of independent and constrained refinement
 $\Delta\rho_{\max} = 0.40 \text{ e } \text{Å}^{-3}$
 $\Delta\rho_{\min} = -0.24 \text{ e } \text{Å}^{-3}$

Compound (IV)

Crystal data

$\text{C}_7\text{H}_9\text{N}_2^+ \cdot \text{C}_4\text{H}_2\text{N}_3\text{O}_4^-$
 $M_r = 277.25$
 Triclinic, $P\bar{1}$
 $a = 4.3625 (4) \text{ Å}$
 $b = 10.4461 (11) \text{ Å}$
 $c = 13.8556 (12) \text{ Å}$
 $\alpha = 78.551 (7)^\circ$
 $\beta = 86.841 (8)^\circ$
 $\gamma = 84.051 (7)^\circ$
 $V = 615.13 (10) \text{ Å}^3$
 $Z = 2$
 Mo $K\alpha$ radiation
 $\mu = 0.12 \text{ mm}^{-1}$
 $T = 298 \text{ K}$
 $0.15 \times 0.08 \times 0.05 \text{ mm}$

Table 4
Hydrogen-bond geometry (Å, °) for (III).

D—H...A	D—H	H...A	D...A	D—H...A
N1—H1...O5 ⁱ	0.91 (2)	1.92 (2)	2.8359 (16)	178 (2)
N3—H3...O2 ⁱⁱ	0.90 (2)	1.97 (2)	2.8635 (16)	178 (2)
N4—H4A...O2	0.84 (2)	2.19 (2)	2.8581 (16)	135.5 (19)
N4—H4A...O3	0.84 (2)	2.12 (2)	2.8808 (18)	150 (2)
N4—H4B...O1 ⁱⁱⁱ	0.88 (2)	1.98 (2)	2.8514 (18)	168 (2)
N5—H5A...O3	0.85 (3)	2.19 (3)	2.9250 (19)	146 (2)
N5—H5B...O7 ⁱⁱⁱ	0.88 (3)	2.18 (3)	3.035 (2)	164 (2)
O6—H61...O4	0.91 (5)	2.00 (5)	2.894 (2)	167 (4)
O6—H62...O4 ^{iv}	0.78 (4)	2.29 (4)	3.037 (3)	160 (4)
O7—H71...O6	0.89 (3)	1.84 (3)	2.729 (3)	173 (3)
O7—H72...O7 ⁱⁱⁱ	0.87 (4)	2.04 (4)	2.8940 (19)	169 (4)

Symmetry codes: (i) $-x + 1, -y + 2, -z + 2$; (ii) $-x, -y + 1, -z + 2$; (iii) $-x + \frac{1}{2}, y - \frac{1}{2}, -z + \frac{1}{2}$; (iv) $x, y - 1, z$.

Table 5
Hydrogen-bond geometry (Å, °) for (IV).

D—H...A	D—H	H...A	D...A	D—H...A
N3—H3...O2 ⁱ	0.92 (3)	1.98 (3)	2.899 (2)	176 (2)
N4—H4A...O1	0.92 (3)	2.07 (3)	2.890 (3)	148 (3)
N4—H4B...N1 ⁱⁱ	0.87 (3)	2.03 (3)	2.886 (3)	170 (2)
N5—H5A...O1	0.89 (3)	2.05 (3)	2.853 (3)	149 (2)
N5—H5B...O3 ⁱ	0.86 (3)	2.23 (3)	3.084 (3)	169 (2)

Symmetry codes: (i) $-x + 1, -y + 2, -z$; (ii) $-x, -y + 1, -z$.

Data collection

Oxford Xcalibur S CCD area-detector diffractometer
 Absorption correction: multi-scan [CrysAlis RED (Oxford Diffraction, 2006); empirical (using intensity measurements) absorption correction using spherical harmonics implemented
 in the SCALE3 ABSPACK scaling algorithm
 $T_{\min} = 0.978, T_{\max} = 0.993$
 4864 measured reflections
 2153 independent reflections
 1427 reflections with $I > 2\sigma(I)$
 $R_{\text{int}} = 0.034$

Refinement

$R[F^2 > 2\sigma(F^2)] = 0.051$
 $wR(F^2) = 0.119$
 $S = 1.05$
 2153 reflections
 201 parameters
 H atoms treated by a mixture of independent and constrained refinement
 $\Delta\rho_{\max} = 0.18 \text{ e } \text{Å}^{-3}$
 $\Delta\rho_{\min} = -0.17 \text{ e } \text{Å}^{-3}$

All H atoms were found in a difference map. The H atoms of the benzene rings were positioned with idealized geometry and refined isotropically as riding on their parent atoms, with C—H = 0.97 Å and $U_{\text{iso}}(\text{H}) = 1.2U_{\text{eq}}(\text{C})$. All other H atoms, including those of the water molecules, were refined freely. In the case of BenzamH⁺·Isor⁻, (II), the refinement converged at a rather high R value, despite the residuals in the final difference map being comparable in this compound with those of compounds (I), (III) and (IV); the crystal quality for (II) was not high, as indicated by the merging index of 0.073. Apparently, the reason why it was not possible to attain an R value lower than 0.087 refers to significant difficulties in selecting a better crystal to improve the experimental data. The crystals of (II) normally form aggregates from water and several attempts undertaken to obtain better results from alternative polar solvents gave no crystalline material. However, the data set collected for compound (II) appeared satisfactory, as judged by the data completeness (99.7% at $\theta = 32.0^\circ$). Scrutiny of the resulting interatomic distances and the U^{ij} values in compound (II), and comparison with the corresponding geometrical parameters in compounds (I), (III) and (IV) showed no anomalies. In

the case of BenzamH⁺·Nit⁻, (IV), diffraction from the very small crystals was weak. Nevertheless, these data gave good structural results, albeit with a lower data/parameter ratio than usual.

For all four compounds, data collection: *CrysAlis CCD* (Oxford Diffraction, 2006); cell refinement: *CrysAlis RED* (Oxford Diffraction, 2006); data reduction: *CrysAlis RED*; program(s) used to solve structure: *SIR97* (Altomare *et al.*, 1999); program(s) used to refine structure: *SHELXL97* (Sheldrick, 2008); molecular graphics: *ORTEP-3* (Farrugia, 1997); software used to prepare material for publication: *WinGX* (Farrugia, 1999).

The author thanks MIUR (Rome) for 2006 financial support of the project 'X-ray diffractometry and spectrometry'.

Supplementary data for this paper are available from the IUCr electronic archives (Reference: FN3053). Services for accessing these data are described at the back of the journal.

References

- Allen, F. H. (2002). *Acta Cryst.* **B58**, 380–388.
- Allen, F. H., Motherwell, W. D. S., Raithby, P. R., Shields, G. P. & Taylor, R. (1999). *New J. Chem.* **23**, 25–34.
- Altomare, A., Burla, M. C., Camalli, M., Cascarano, G. L., Giacovazzo, C., Guagliardi, A., Moliterni, A. G. G., Polidori, G. & Spagna, R. (1999). *J. Appl. Cryst.* **32**, 115–119.
- Barker, J., Phillips, P. R., Wallbridge, M. G. H. & Powell, H. R. (1996). *Acta Cryst.* **C52**, 2617–2619.
- Bernstein, J., Davis, R. E., Shimoni, L. & Chang, N.-L. (1995). *Angew. Chem. Int. Ed. Engl.* **34**, 1555–1573.
- Bernstein, J., Etter, M. C. & Leiserowitz, L. (1994). *Structure Correlation*, Vol. 2, edited by H.-B. Bürgi & J. D. Dunitz, pp. 458–463. Weinheim: VCH.
- Bis, J. A., Vishweshwar, P., Weyna, D. & Zaworotko, M. J. (2007). *Mol. Pharm.* **4**, 401–416.
- Childs, S. L., Stahly, G. P. & Park, A. (2007). *Mol. Pharm.* **4**, 323–338.
- Etter, M. C. (1990). *Acc. Chem. Res.* **23**, 120–139.
- Etter, M. C., MacDonald, J. C. & Bernstein, J. (1990). *Acta Cryst.* **B46**, 256–262.
- Farrugia, L. J. (1997). *J. Appl. Cryst.* **30**, 565.
- Farrugia, L. J. (1999). *J. Appl. Cryst.* **32**, 837–838.
- Ferretti, V., Bertolasi, V. & Pretto, L. (2004). *New J. Chem.* **28**, 646–651.
- Gagnon, E., Maris, T., Maly, K. R. & Wuest, J. D. (2007). *Tetrahedron*, **63**, 6603–6613.
- Gilli, G. & Gilli, P. (2009). *The Nature of the Hydrogen Bond*, pp. 163–167. Oxford University Press.
- Gregson, R. M., Glidewell, C., Ferguson, G. & Lough, A. J. (2000). *Acta Cryst.* **B56**, 39–57.
- Grzesiak, A., Helland, R., Smalas, A. O., Krowarsch, D., Dadlez, M. & Otlewski, J. (2000). *J. Mol. Biol.* **301**, 205–217.
- Herbstein, F. H. (2005). *Crystalline Molecular Complexes and Compounds*, Vol. 2, pp. 908–911. Oxford University Press.
- Johnson, S. L. & Rumon, K. A. (1965). *J. Phys. Chem.* **69**, 74–86.
- Jokić, M., Bajić, M., Žinić, M., Perić, B. & Kojić-Prodić, B. (2001). *Acta Cryst.* **C57**, 1354–1355.
- Kojić-Prodić, B. & Molčanov, K. (2008). *Acta Chim. Slov.* **55**, 692–708.
- Kolev, T., Koleva, B. B., Seidel, R. W., Spittler, M. & Sheldrick, W. S. (2009). *Struct. Chem.* **20**, 533–536.
- Kolotuchin, S. V., Fenlon, E. E., Wilson, S. R., Loweth, C. J. & Zimmerman, S. C. (1995). *Angew. Chem. Int. Ed. Engl.* **34**, 2654–2657.
- Kratochvíl, B., Ondráček, J., Krechl, J. & Hašek, J. (1987). *Acta Cryst.* **C43**, 2182–2184.
- Leiserowitz, L. (1976). *Acta Cryst.* **B32**, 775–802.
- Li, X., He, X., Wang, B. & Merz, K. (2009). *J. Am. Chem. Soc.* **131**, 7742–7754.
- Molčanov, K. & Kojić-Prodić, B. (2010). *CrystEngComm*, **12**, 925–939.
- Motherwell, W. D. S., Shields, G. P. & Allen, F. H. (1999). *Acta Cryst.* **B55**, 1044–1056.
- Nangia, A. & Desiraju, G. R. (1998). *Top. Curr. Chem.* **198**, 57–95.
- Oxford Diffraction (2006). *CrysAlis CCD* and *CrysAlis RED*. Versions 1.171.32.3. Oxford Diffraction Ltd, Abingdon, Oxfordshire, England.
- Pereira Silva, P. S., Domingos, S. R., Ramos Silva, M., Paixão, J. A. & Matos Beja, A. (2008). *Acta Cryst.* **E64**, o1082–o1083.
- Portalone, G. (2008a). *Acta Cryst.* **E64**, o1282–o1283.
- Portalone, G. (2008b). *Acta Cryst.* **E64**, o656.
- Portalone, G. & Colapietro, M. (2007a). *Acta Cryst.* **C63**, o181–o184.
- Portalone, G. & Colapietro, M. (2007b). *Acta Cryst.* **C63**, o650–o654.
- Portalone, G. & Colapietro, M. (2009). *J. Chem. Crystallogr.* **39**, 193–200.
- Powers, J. C. & Harper, J. W. (1999). *Proteinase Inhibitors*, edited by A. J. Barrett & G. Salvesen, pp. 55–152. Amsterdam: Elsevier.
- Robinson, J. M. A., Philp, D., Harris, K. D. M. & Kariuki, B. M. (2000). *New J. Chem.* **24**, 15–24.
- Sarma, B., Nath, N. K., Bhogala, B. R. & Nangia, A. (2009). *Cryst. Growth Des.* **9**, 1546–1557.
- Shattock, T. R., Arora, K. K., Vishweshwar, P. & Zaworotko, M. J. (2008). *Cryst. Growth Des.* **8**, 4533–4545.
- Sheldrick, G. M. (2008). *Acta Cryst.* **A64**, 112–122.
- Thallapally, P. K., Basavoju, S., Desiraju, G. R., Bagieu-Beucher, M., Masse, R. & Nicoud, J.-F. (2003). *Curr. Sci.* **85**, 995–1001.
- Thomas, R., Srinivasa Gopalan, R., Kulkarni, G. U. & Rao, C. N. R. (2005). *Beilstein J. Org. Chem.* **1**, 799–806.
- Tidwell, R. R. & Boykin, D. W. (2003). *DNA and RNA Binders: From Small Molecules to Drugs*, Vol. 2, edited by M. Demeunynck, C. Bailly & W. D. Wilson, pp. 414–460. Weinheim: Wiley-VCH.
- Ward, M. D. (2005). *Chem. Commun.* pp. 5838–5842.